

Improving Recycling of Polyethylene-Coated Paperboard with a Nanofibrillated Cellulose Layer

Mohammed Z. Al-Gharrawi,^a Jinwu Wang,^b and Douglas W. Bousfield ^a

To improve the ability to recycle polyethylene (PE)-coated paperboard, one solution may be to use nanofibrillated cellulose (NFC) to generate a layer that should weaken when wet that leads to a clean separation between the polymer film and the pulp fibers. This NFC layer has the potential to improve the package's oxygen and grease barrier properties, but this system has not been explored in the literature. In this study, papers coated with zero, 2, and 4 g/m² of NFC were laminated with a PE film under a range of pressing temperatures and times at a constant pressing pressure. A model was developed to predict fiber recovery given the air permeability of the paper, pressing time, polymer temperature, and paper void volume. The recyclability or fiber recovery was evaluated in addition to the adhesive strength. Samples with the NFC layer had much improved fiber recovery because the NFC layer gives a good separation during the recycling operation. The model predictions were compared to the experiments.

Keywords: Food packaging; Cellulose nanofibers; Recycling; Polyethylene coated paper; Repulping; Barrier coatings

Contact information: a: Department of Chemical and Biomedical Engineering, University of Maine, Orono, ME 94469 USA; b: Forest Products Laboratory, U.S. Forest Service, 1 Gifford Pinchot Drive, Madison, WI 53726, USA; Corresponding author: bousfld@maine.edu

INTRODUCTION

Polyethylene (PE)-coated paperboard is a conventional method to produce packaging containing liquid products such as paper cups, aseptic packaging, and juice cartons. Compared with plastic, metal, and glass based options, PE-coated paperboard should have a better life cycle analysis and environmental impact, especially if this packaging can be recycled. However, PE-coated paperboard is difficult to recycle due to the PE film that is attached to the paper fibers. A significant percentage of the fiber is embedded in the PE film and is not recovered at the re-pulping stage. This issue results in PE material with a low value and reduces fiber recovery: these issues were the motivation for the “NextGen cup challenge”. Triantafillopoulos and Koukoulas (2020) discuss issues around composting and recycling of single-use paper cups. While many solutions are of high interest, there is still a need to understand various methods to improve these systems' ability to be recycled.

Many patents and papers discuss PE-coated paperboard production and recycling these products (*e.g.* Wenzel *et al.* 1998; Hopewell *et al.* 2009; Sharma *et al.* 2019). PE is usually extrusion-coated onto the board by contacting the molten polymer to the paper, followed by a cold pressure nip. In the nip, PE is pressed against the paper surface to insure good contact and adhesion. This pressure also causes the PE to intermix with the fibers, incorporating a certain percent of the fibers into the polymer matrix. While this does cause

the final product to be impervious to water and water vapor, it also creates an issue related to effective recycling of the material.

The recycling of paper and plastic waste is a promising way to achieve a zero-waste goal. However, the separation of plastics from other materials is still challenging and limits the amount of plastics that can be recycled through modern sorting technologies (Srivatsa and Markham 1993; Sharma *et al.* 2019). The number of plastic types is another challenge for the recycling sector to achieve effective recycling; new bioplastics only add to this challenge. Moreover, the incompatibility of plastic types with each other makes the production of recycled resins from plastic waste a challenging activity (Hopewell *et al.* 2009; Sharma *et al.* 2019).

The recycling rate of plastics for re-use in food packaging is low due to issues around clean and pure sources of post-consumer plastics (Arvanitoyannis and Bosnea 2001). While many producers would like to move towards packaging that uses more recycled materials, the clean separation of adhesive, paper, and other contaminants is difficult. When PE is coated onto paper or paperboard, a fraction of the paper fibers become incorporated into the PE film. This results in less fiber available to recover and a PE material that contains paper fibers intermixed.

One possible solution to recycling PE coated paperboard is to use nanofibrillated cellulose (NFC) or microfibrillated cellulose (MFC) as a release layer between PE and paper. NFC suspensions (which are also called CNF suspensions), when applied to paper, form a dense layer. Blade coating and slot dye coating of NFC has been demonstrated, and the resulting cross sections show an impressive dense layer on the paper surface (Kumar *et al.* 2016, 2017; Mousavi *et al.* 2017, 2018). NFC can also be applied on the wet-end of a paper machine as a top layer (Johnson *et al.* 2019). The key idea is that this NFC layer will prevent the deep penetration of PE film into the paper, resulting in a clean separation of PE from the paper in a basic paper recycling system. The NFC layer is known to lose mechanical properties when wet, but when dry, it has impressive mechanical properties. Therefore, the NFC layer should have good mechanical properties when used in the package, but in a recycling system, it should lose its strength and become part of the fiber stream. Figure 1 depicts the key idea of this system. Some amount of the NFC may be incorporated into the PE film, but this is expected to be a small amount. Future studies may need to characterize the amount of NFC in the PE film and the influence of this issue on the quality and ability to reuse the PE film. However, this situation is improved from the current situation in which a significant amount of the paper fibers become incorporated with the PE film.

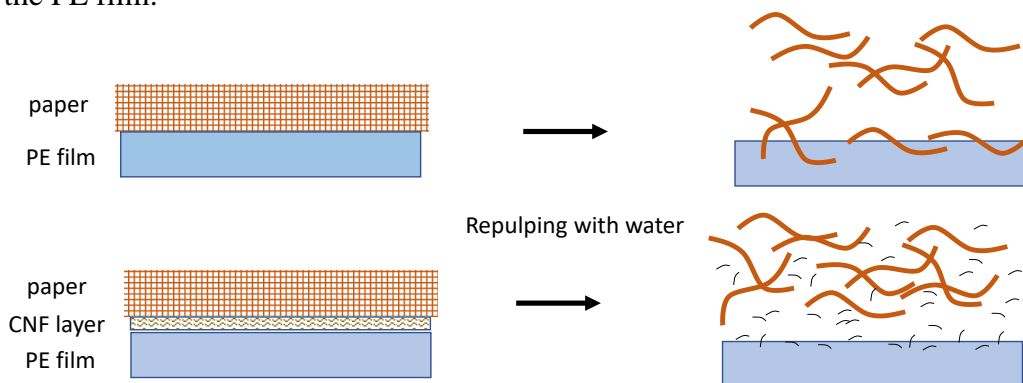


Fig. 1. Concept of NFC layer to promote a clean separation of PE film from base paper in recycling operation

A NFC layer may have other beneficial properties. NFC films are known to be an excellent oxygen and grease barrier. Several groups have published the excellent oxygen resistance of cellulose nanomaterials (Fukuzumi *et al.* 2009; Syverud and Stenius 2009; Aulin *et al.* 2010; Hult *et al.* 2010; Plackett *et al.* 2010). The oxygen transmission rates (OTR) for pure NFC without any additive as low as $17 \text{ mL m}^{-2} \text{ day}^{-1}$ were obtained for films prepared from $30 \text{ }\mu\text{m}$ thick pure NFC (Syverud and Stenius 2009). The potential to use NFC and the related moisture and oxygen permeabilities is reviewed by Lavoine *et al.* (2012) and Wang *et al.* (2018). In another kind of NFC, the oxygen permeability significantly decreases by a couple orders of magnitude with a $0.4 \text{ }\mu\text{m}$ thick layer of TEMPO-oxidized cellulose nanofibers on a $25 \text{ }\mu\text{m}$ thick polylactic acid (PLA) film (Fukuzumi *et al.* 2009). Koppolu *et al.* (2019) demonstrated that paper with a NFC layer coated with PLA results in good barrier properties. Therefore, a package system of paper-NFC-PE should have good barrier properties for both oxygen and water vapor. In addition, this system may also result in a clean separation between PE and the fibers in a typical recycling system because the NFC layer should weaken upon contact with water. This type of packaging system has not been reported in the literature.

This work investigates the potential of using NFC as a layer in a PE-NFC-Paper system to improve the recycling operation. PE films are laminated to NFC-coated paper at various temperatures and pressing times. A method to characterize the recovery of fibers is developed. A simple model is proposed to predict the fiber recovery. Also, the adhesive strength of the PE to the samples is measured.

EXPERIMENTAL

Three base papers with 80 g/m^2 basis weight were used in this work: one had no NFC, while the other two had 2 and 4 g/m^2 as a top layer of cellulose nanofibers. The base sheet was an 80:20 hardwood: softwood blend. The paper was manufactured on a pilot paper machine at the University of Maine Process Development Center, which consists of a Fourdrinier forming section, press section, and drying section. The NFC used in this study was produced from bleached softwood kraft pulp by two-stage disk refining at 3% consistency with specialized plates, to a fines content of 90% as measured on a fiber size analyzer (MorFI, Techpap Inc.). This NFC has a large number of fibrils that are on the order of 50 nm in diameter and $5 \text{ }\mu\text{m}$ in length, but there is a large size distribution of material.

The surface application of NFC on paper was achieved with an in-house built secondary headbox. The NFC suspension is diluted to 0.5% solids, and its flow rate was adjusted to form a curtain of the suspension that lands around one meter after the headbox. The amount of NFC that ends up on the paper is adjusted by the flow rate of the NFC suspension to the machine. The water from the NFC suspension is removed in the table section of the machine. The paper and the NFC layer go through a normal two-nip press section and is dried with steam heated rolls.

The paper properties were characterized in a number of ways. The base paper had a basis weight of 80 g/m^2 . The thickness of the paper was measured with a digital micrometer (Marathon) with a resolution of $1 \text{ }\mu\text{m}$. The bulk density reported in terms of specific density of the samples ranged from 1.3 to $1.35 \text{ cm}^3/\text{g}$. The thicknesses of the samples were all similar at 0.10 mm . The NFC-coated paper had a low permeability

compared to the base paper without the NFC layer: the permeability coefficients of the papers that had 0, 2, and 4 g/m² of NFC on the surface were 1×10^{-14} , 3×10^{-15} , and 1×10^{-16} m², respectively, based on the air permeability tests reported Johnson *et al.* (2019). The rate of water uptake for the coated paper was over ten times slower on the NFC coated side than the uncoated paper. More details about the method to produce the papers and the paper properties are given in Johnson *et al.* (2019).

The void fraction of the paper was measured by the silicon oil void test described by Rioux (2003),

$$\varepsilon = \frac{(W_o - W_d)}{\rho AT} \quad (1)$$

where W_o and W_d are oil-saturated and dry paper weight, respectively, ρ is the density of silicon oil, A is the area of the sample, and T is the thickness of the sample. The void fractions of the three papers were all around 0.34. This value is lower than the void fraction that would be calculated based on the bulk density that indicates a void fraction of 0.47. This difference may be related to the ability of the silicon oil to fully penetrate these samples or other issues related to the measurements of thickness of the sample.

Low-density polyethylene (LDPE) films from (McMaster-Carr, Princeton, NJ, USA), with a thickness of 51 μ m, were cut into 127 x 127 mm squares. Aluminum foil and the paper sample were also cut to these dimensions. The foil keeps the sample from sticking to the heated block in the hot press (Carver, model: C 41000-003, Wabash, IN, USA). The foil and PE film were first placed on the lower block for one minute to allow the sample to obtain the set temperature of the block. A cylinder was rolled on the top of PE to eliminate any wrinkles that may result from air bubbles. The paper sample, with the NFC layer down toward the PE film, was set on top. The hot press was already at the desired temperature. The press was activated to press for the desired time, here either 10 or 30 seconds. The pressure inside the air cylinder that actuates the press was set to 0.27 MPa. After accounting for the cross-sectional area of the cylinder and the sample, the pressure applied to the samples should be 0.24 MPa. After releasing, the sample was removed and cooled at room temperature. The foil becomes part of the sample but is peeled away. Figure 2 illustrates the pressing event. While these stages are quite different from the extrusion coating of paperboard, the procedure employed should simulate the basic process on a lab scale.

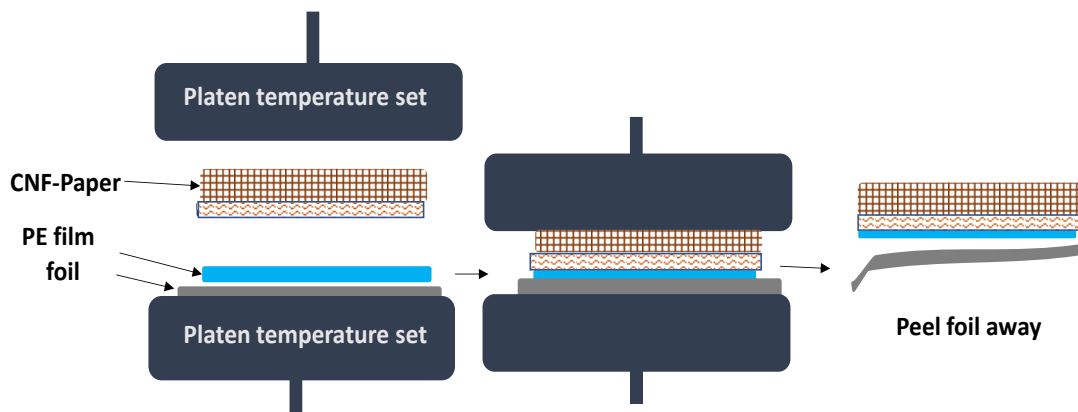


Fig. 2. Lamination of PE on the paper. PE is heated to target pressure. Paper is placed on the PE film and the press is activated. Foil peeled afterwards.

Figure 3 depicts the procedure to measure fiber recovery. The laminated PE-paper is cut into 16 square pieces (25.4 x 25.4 mm), and they are put in a beaker with 250 mL of water. The contents are mixed with an overhead stirrer (IKA RW20 Digital, Wilmington, DE, USA) at 620 rpm for 15 min and allowed to soak for 24 h. The suspension is screened with an opening size of 3.36 mm to separate the PE film from suspended fibers. The dry weight of the PE film before contact is known from its basis weight and the area used. The change in the dry weight of the PE film is used to calculate the mass of fibers that are embedded in the PE layer; this would be the mass of fibers that would not be recovered in a recycling system. The fiber recovery factor is the mass of fibers not embedded in the PE film divided by the initial mass of fibers, which includes the mass of the NFC. In an actual paper recycling system, the recovery may be different than this value, but this method should give an approximate idea as to how easy the PE film is separated from the paper fibers.

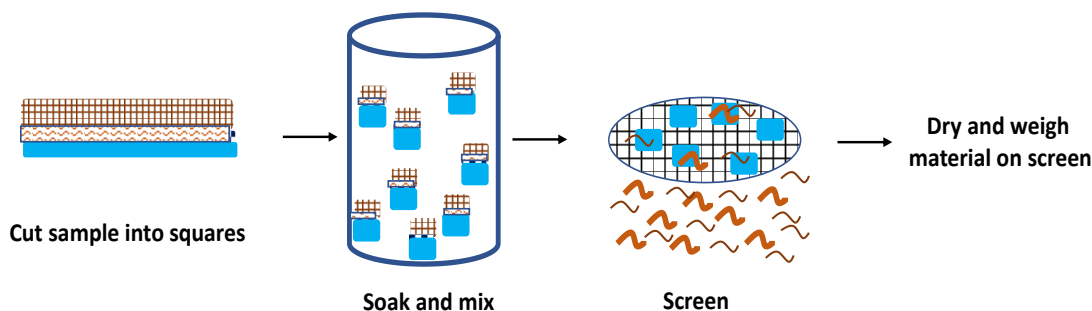


Fig. 3. Steps or stages of recycling of laminated PE-NFC-paper

The actual sample area was 10×15 cm. In the pressing step, an area of 10×10 cm was used to leave a region not bonded to the PE film. The PE-paper samples were cut into 12 mm wide and 15 cm long strips. These unbounded regions are clamped into the grips of a mechanical tester (model 5564, INSTRON, Norwood, MA, USA). The peeling occurs at 180° as the paper-PE region is peeled from the paper at a rate of 2 mm/min. The force and displacement are recorded.

Theory and Modeling

A model for polymer penetration into the paper was developed based on Darcy's law for flow through a porous medium. The specific volumetric flow rate is related to the pressure drop ΔP , permeability of the paper k , viscosity of the fluid μ , and the distance of penetration L as follows.

$$\frac{dV}{dt} = \frac{\Delta P k A}{\mu L} \quad (2)$$

A mass balance links the volume that has penetrated into the paper with the penetration depth as $V = AL\varepsilon$, where ε is the void fraction of the paper. Inserting this mass balance into Eq. 2 and integrating in time, a simple expression for the penetration depth can be obtained as shown in Eq. 3.

$$L = \sqrt{\frac{2\Delta P k t}{\mu \varepsilon}} \quad (3)$$

The pressure to use should be the press pressure as delivered from the force in the press divided by the sample area. The time is the pressing time used in the experiment. The paper's permeability coefficient was measured with the Gurley tester, as described in Johnson *et al.* (2019). The Gurley tester measures the time for 100 mL of air to flow through 1 in² area of the sample with a pressure of 1200 Pa. Knowing the thickness of the sample and the viscosity of air, a permeability can be calculated. A key assumption of the model is that the permeability of the sample should be the same for air and for the molten PE.

For a certain penetration depth, knowing the thickness of the paper, the fiber recovery can be estimated. For example, if the penetration depth is calculated to be 20 μm and the paper thickness is 100 μm , the recovery would be 80%.

The key parameter is the viscosity of the polymer at its application temperature. In this case, the polymer starts as a film; it is not clear how to prepare the sample for a rheological test. However, in the literature, the viscosity of linear low-density polyethylene is reported. An expression is given for the viscosity of polyethylene as a function of temperature as Zatloukal (2016),

$$\ln(\mu) = \frac{6284}{T} - 5.7 \quad (4)$$

where μ is the Newtonian viscosity (Pa s), and T is the temperature ($^{\circ}\text{K}$). Therefore, for a certain temperature, the viscosity can be estimated with Eq. 4 and used in Eq. 3 to predict the penetration, that in turn, can be used to estimate fiber recovery.

RESULTS AND DISCUSSION

The fiber recovery factor as a function of the pressing temperature is given in Fig. 4 for the paper sample with no NFC and 2 and 4 g/m^2 NFC layer for a pressing time of 10 seconds. Each condition was repeated three times with a standard deviation of around 8%.

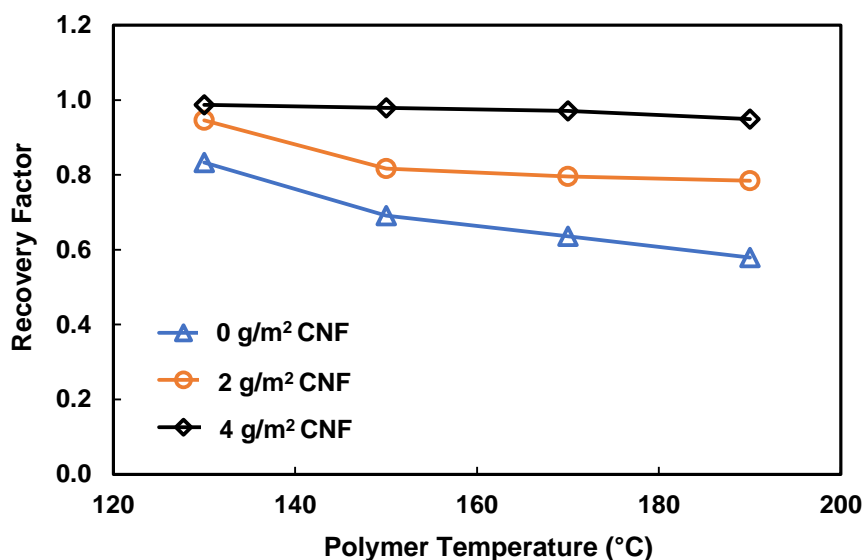


Fig. 4. Recover factor of paper coated with NFC at 0, 2, and 4 g/m^2 for different polymer temperatures at pressing time 10 seconds

For the uncoated paper sample, as the temperature of the polymer was increased, the viscosity decreased, leading to an increase in penetration of the polymer into the paper. This increase in penetration decreased the fiber recovery factor. For a temperature of 190 °C, the recovery factor was in the range of 60% for the uncoated paper. For the 2 g/m² NFC sample, a similar trend was seen, yet the fiber recovery factors were larger than the uncoated sample, increasing to 80% for the high temperature. For the 4 g/m² NFC sample, the fiber recovery factor was over 95% for all temperatures. This shows the ability of the NFC layer to stop the penetration of polymer into the paper and help the polymer release from the sample in wet conditions.

The results for 30-second pressing are shown in Fig. 5. Similar trends were seen compared with the shorter pressing time. Even at high temperatures, the NFC layers resulted in almost complete recovery of the fibers. For the uncoated papers sample, the recovery dropped to under 50%. The 2 g/m² samples, for some reason, were closer to the 4 g/m² samples for the 30-second press than the 10 second press time. The longer press time may release water vapor from the paper, which generates some pressure that hinders the penetration of the polymer for this situation. Both pressing times clearly show the excellent fiber recovery for sample coated even with 2 g/m² and a decrease in recovery with higher temperatures.

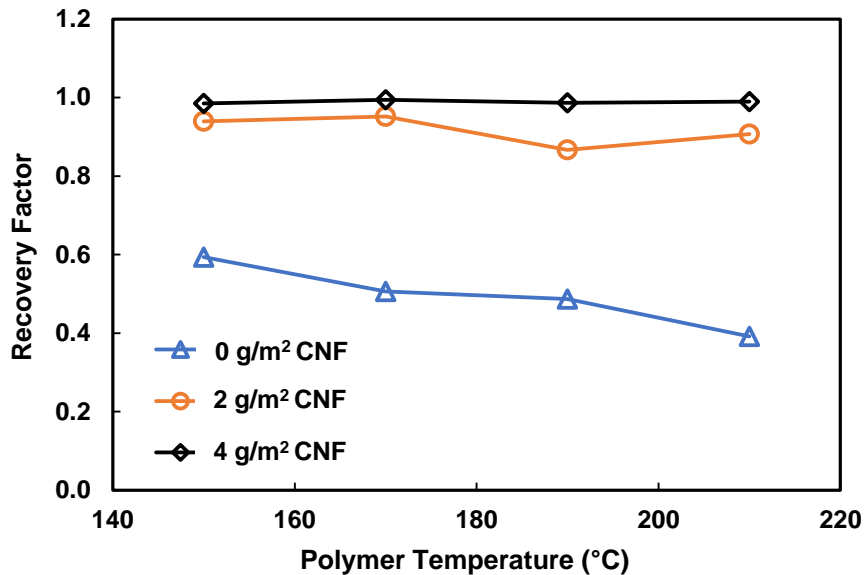


Fig. 5. Recover factor of paper coated with NFC at 0, 2, and 4 g/m² for different polymer temperatures at pressing time 30 seconds

The predicted penetration depth in Eq. 3 was used to estimate the amount of fiber that would not be recovered. Because the polymer viscosity value at the shear rate obtained in the pore space is unknown, the potential pore space changes upon contact with a molten polymer, and other approximations of the model, a calibration factor, is needed for Eq. 3. Accordingly, Eq. 3 is modified as shown in Eq. 5.

$$L = \sqrt{\frac{2C\Delta Pkt}{\mu\varepsilon}} \quad (5)$$

The factor C is used to account for uncertain parameters and assumptions in the model such as the true viscosity of the polymer at the temperature inside the pore, the permeabilities that were obtained from air flow but may be different for a polymer with a pressure gradient, and the true pressure that is applied to the sample. Figures 6 and 7 show the predicted fiber recovery when C is set to a value of 200. For example, using the paper permeability of $1 \times 10^{-14} \text{ m}^2$, a viscosity of 2600 Pa s at 190 °C, a void fraction of 0.34, a press time of 10 s, and a pressure of 240 kPa, the penetration depth was 35 μm . For a paper thickness of 103 μm , the recovery factor was then 0.66. This value was not far from the experimental result. For the 30 s press time at 210 °C, the predicted recovery factor was 0.4, and the measured value was 0.38.

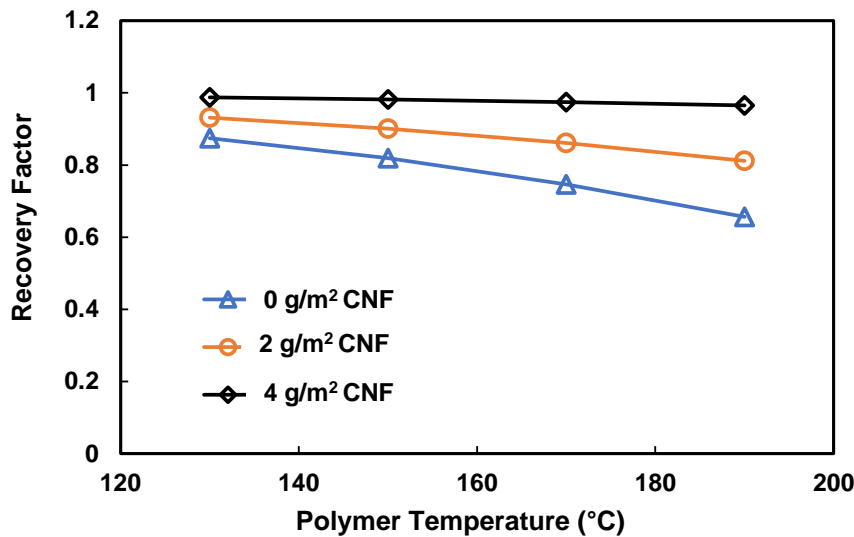


Fig. 6. Predicted recovery factor of paper for 0, 2, and 4 g/m² NFC on paper samples at different temperatures for pressing time 10 seconds with $C=200$

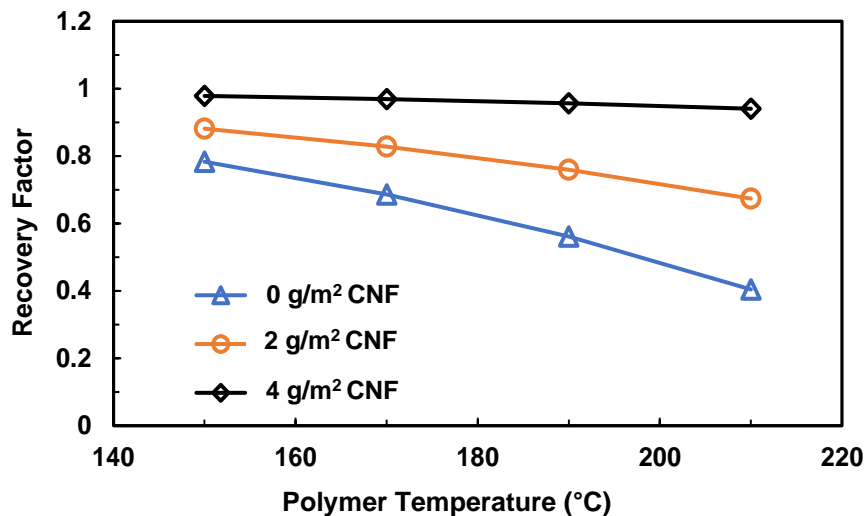


Fig. 7. Predicted recover factor of paper for 0, 2, and 4 g/m² NFC on paper for different temperatures for pressing time 30 seconds with $C=200$.

The void fraction used in the predictions is that of the paper with the NFC layer. For the NFC coated paper, the void fraction that should be used is that of the NFC layer. Recently, others have measured the void fraction of NFC films, obtaining results in the range of 0.4 to 0.5 (Fein 2020). These values are high in view of some low magnification SEM images of cut samples, but these have been measured in various ways. Therefore, the error caused by using the bulk porosity is around 30%. The true porosity of the NFC layer on these papers is difficult to characterize.

Even though the calibration factor is larger than expected, the expression picks up the trends in the data quite well. For different paper samples, temperatures, and pressing times, the correct trends are predicted. This result indicates that the basic mechanisms of the pressing event are captured by the expression and the temperature-dependent viscosity. Figure 8 compares the predicted and measured fiber recovery factors for all the polymer temperatures, paper samples, and pressing time. The only set of results that do not fit well along the 45-degree line are the 2 g/m² NFC samples at the 30 s pressing times.

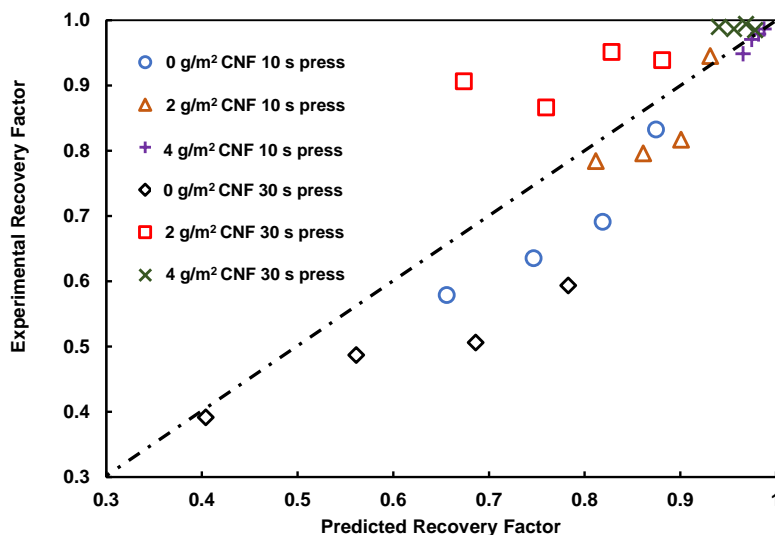


Fig. 8. Predicted and measured fiber recovery factors for all temperatures and pressing times with $C=200$

Peel resistance of adhesive (T-Peel Test) was applied to the samples. The steady state load was recorded for the peeling event. Figures 9 and 10 show the results for the 10 and 30 second pressing times, respectively. Adding NFC to the paper surface weakens the adhesion forces by an order of magnitude. For the papers with no NFC, fiber tear is seen in the test, and the force measured is a function of the paper strength. In the case of 30-second pressing, the adhesive force of 2 g/m² NFC surface paper is only twenty percent of the paper with no NFC. Adding more NFC leads even smaller peeling force. This result is not surprising in that the NFC layer blocks most penetration of the polymer into the structure and prevents bonding by mechanical interlocking. Therefore, the same mechanism that helps lead to improved recycling of the PE coated paperboard also leads to poor adhesion. The tensile and compression properties of these samples are not expected to change because of the NFC layer.

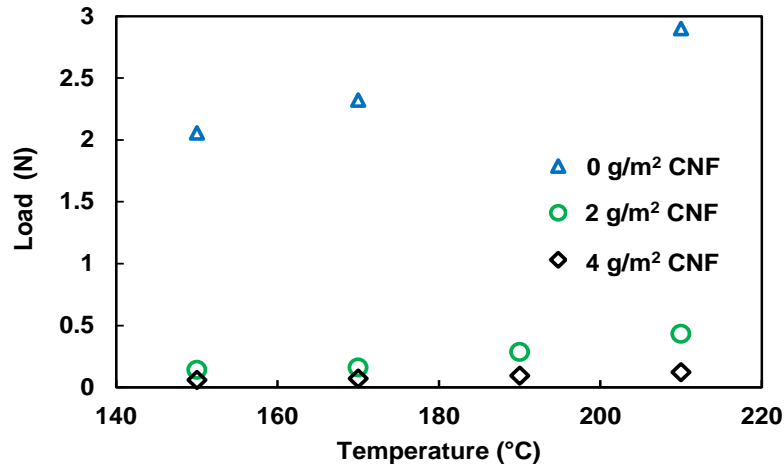


Fig. 9. Steady peeling load measured for 10 second pressing for 0, 2, and 4 g/m² NFC on paper

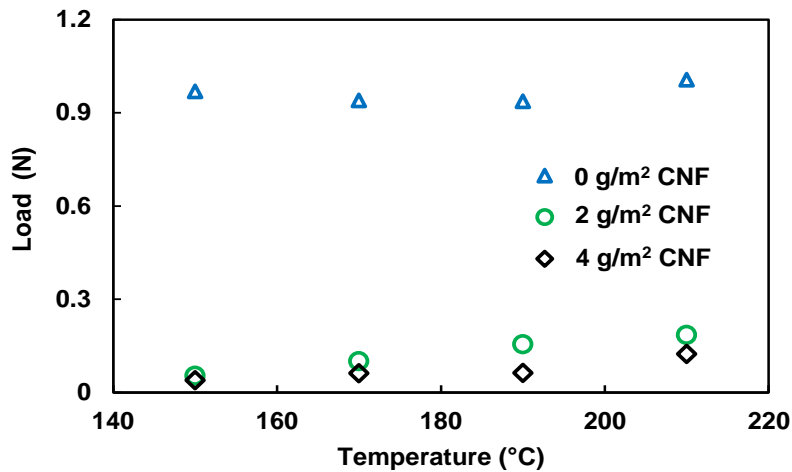


Fig. 10. Steady peeling load measured for 30 second pressing for 0, 2, and 4 g/m² NFC on paper

The moisture barrier properties of the paper with a NFC layer are poor. The NFC layer adds little resistance to the diffusion of water through the sample. The water vapor transmission rates are over 400 g/m² day. Once the PE layer is added, the transmission rates drop to values that are too low to measure in a reasonable time frame. The values are less than 0.1 g/m² day. This result is expected because of the impressive barrier properties to moisture of polyethylene.

The reason that NFC layers have good oxygen and oil/grease barrier properties is not clear in the literature. The mechanically produced NFC can have oxygen barrier properties that are similar or even better than high quality forms of NFC (Kumar *et al.* 2014). Fein (2020) shows that as NFC layers dry, they tend to form a layered structure that are able to withstand a folding event and still have good oil barrier properties; these layer structures do have large pores but it seems like these pore are not connected in the thickness direction. Tayeb *et al.* (2020a) show that even lignin containing NFC (LNFC) produced from unbleached pulps had good oxygen and oil barrier properties. Österberg *et al.* (2013) and Tayeb *et al.* (2020b) show that hot pressing of films can improve the oxygen barrier properties and improve their sensitivity to moisture. These oil barrier properties also may

be related to the ability of the NFC layer to block the penetration of molten polymer in the pressing step. The oxygen transmission rate of the paper with NFC layer used here was too high to be measured with the standard device. This result is linked to the thin layer of NFC used. Tayeb *et al.* (2020b) show that oxygen transmission rates of the order of 3 to 10 cm³/m² day for films of NFC that were 70 g/m² basis weight using the same NFC; some tests with PE films showed that humidity did not degrade the oxygen barrier properties for these films. Kumar *et al.* (2014) report a rate of 1.5 cm³/m² day for a normalized thickness of 25 μm using the same NFC as used here.

This issue of poor adhesion likely can be overcome by using one of several techniques. A primer layer could be coated on the NFC layer that helps promote some adhesion. Additives into the NFC layer, such as latex polymers or similar additives, or chemical modification of NFC could help promote the adhesion of the PE film (Fein *et al.* 2020a, 2020b). Methods to generate some surface texture or pores are possible. Other surface treatments are common in the industry to help improve PE adhesion such as corona or flame treatment of the surface just before PE extrusion coating. Other options are possible such as water dispersions of PE or using biopolymers such as PLA (Vyorykka *et al.* 2011; Koppolu *et al.* 2019).

CONCLUSIONS

1. The addition of nanofibrillar cellulose (NFC) as a thin layer on the paper helped in the recycling of polyethylene (PE)-coated paperboard by decreasing the amount of the fiber that becomes incorporated into the polyethylene film.
2. The NFC layer limits the penetration of the PE film into the paper and generates a weak layer in the course of repulping operations. Even 2 g/m² application resulted in a significant improvement in fiber recovery compared to the uncoated paper.
3. A simple expression was developed that predicts the fiber recovery factor for a range of polymer temperatures, papers, and pressing times.

ACKNOWLEDGMENTS

This project was funded in part by U.S. Endowment for Forestry and Communities (P³Nano) grant number E17-20 and by the University of Maine Paper Surface Science Program (PSSP). The Higher Committee of Education Development in Iraq also provided support.

REFERENCES CITED

- Arvanitoyannis, I. S., and Bosnea, L. A. (2001). "Recycling of polymeric materials used for food packaging: Current status and perspectives," *Food Reviews International* 17(3), 291-346. DOI: 10.1081/FRI-100104703
- Aulin, C., Gällstedt, M., and Lindström, T. (2010). "Oxygen and oil barrier properties of microfibrillated cellulose films and coatings," *Cellulose* 17(3), 559-574. DOI:

- 10.1007/s10570-009-9393-y
- Fein, K., Bousfield, D. W., and Gramlich, W. M. (2020a). “Thiol-norbornene reactions to improve natural rubber dispersion in cellulose nanofiber coatings,” *Carbohydrate Polymers* 250, 117001. DOI: 10.1016/j.carbpol.2020.117001
- Fein, K., Bousfield, D. W., and Gramlich, W. M. (2020b). “The influence of versatile thiol-norbornene modifications to cellulose nanofibers on rheology and film properties,” *Carbohydrate Polymers* 230, 115672. DOI: 10.1016/j.carbpol.2019.115672
- Fein, K. (2020). *Water-Based Modifications of Cellulose Nanofibrils and Processing Influences on Film Properties*, Ph.D. Dissertation, University of Maine, Orono, ME, USA.
- Fukuzumi, H., Saito, T., Iwata, T., Kumamoto, Y. and Isogai, A. (2009). “Transparent and high gas barrier films of cellulose nanofibers prepared by TEMPO-mediated oxidation,” *Biomacromolecules* 10(1), 162-165. DOI: 10.1021/bm801065u
- Hopewell, J., Dvorak, R., and Kosior, E. (2009). “Plastics recycling: Challenges and opportunities,” *Philosophical Transactions of the Royal Society B: Biological Sciences* 364(1526), 2115-2126. DOI: 10.1098/rstb.2008.0311
- Hult, E. L., Iotti, M., and Lenes, M. (2010). “Efficient approach to high barrier packaging using microfibrillar cellulose and shellac,” *Cellulose* 17(3), 575-586. DOI: 10.1007/s10570-010-9408-8
- Johnson, D. A., Paradis, M., Tajvidi, M., Al-Gharrawi, M., and Bousfield, D. (2019). “Surface application of cellulose microfibrils on paper – Effects of basis weight and surface coverage levels,” in: *TAPPI PAPERCON*, Atlanta GA, USA.
- Koppolu, R., Lahti, J., Abitbol, T., Swerin, A., Kuusipalo, J., and Toivakka, M. (2019). “Continuous processing of nanocellulose and polylactic acid into multilayer barrier coatings,” *ACS Applied Materials & Interfaces* 11(12), 11920-11927. DOI: 10.1021/acsami.9b00922
- Kumar, V., Bollström, R., Yang, A., Chen, Q., Chen, G., Salminen, P., Bousfield, D., and Toivakka, M. (2014). “Comparison of nano- and microfibrillated cellulose films,” *Cellulose* 21(5), 3443-3456. DOI: 10.1007/s10570-014-0357-5
- Kumar, V., Elfving, A., Koivula, H., Bousfield, D., and Toivakka, M. (2016). “Roll-to-roll processed cellulose nanofiber coatings,” *Industrial & Engineering Chemistry Research* 55(12), 3603-3613. DOI: 10.1021/acs.iecr.6b00417
- Kumar, V., Koppolu, V.R., Bousfield, D., and Toivakka, M. (2017). “Substrate role in coating of microfibrillated cellulose suspensions,” *Cellulose* 24(3), 1247-1260. DOI: 10.1007/s10570-017-1201-5
- Lavoine, N., Desloges, I., Dufresne, A., and Bras, J. (2012). “Microfibrillated cellulose—its barrier properties and applications in cellulosic materials: A review,” *Carbohydrate Polymers* 90(2), 735-764. DOI: 10.1016/j.carbpol.2012.05.026
- Mousavi, S. M. M., Afra, E., Tajvidi, M., Bousfield, D. W., and Dehghani-Firouzabadi, M. (2018). “Application of cellulose nanofibril (CNF) as coating on paperboard at moderate solids content and high coating speed using blade coater,” *Progress in Organic Coatings* 122, 207-218. DOI: 10.1016/j.porgcoat.2018.05.024
- Mousavi, S. M., Afra, E., Tajvidi, M., Bousfield, D. W., and Dehghani-Firouzabadi, M. (2017). “Cellulose nanofiber/carboxymethyl cellulose blends as an efficient coating to improve the structure and barrier properties of paperboard,” *Cellulose* 24(7), 3001-

3014. DOI: 10.1007/s10570-017-1299-5
- Österberg, M., Vartiainen, J., Lucenius, J., Hippi, U., Seppälä, J., Serimaa, R. and Laine, J. (2013). "A fast method to produce strong NFC films as a platform for barrier and functional materials," *ACS Applied Materials & Interfaces* 5(11), 4640-4647. DOI: 10.1021/am401046x
- Plackett, D., Anturi, H., Hedenqvist, M., Ankerfors, M., Gällstedt, M., Lindström, T., and Siró, I. (2010). "Physical properties and morphology of films prepared from microfibrillated cellulose and microfibrillated cellulose in combination with amylopectin," *Journal of Applied Polymer Science* 117(6), 3601-3609. DOI: 10.1002/app.32254
- Rioux, R. W. (2003). *The Rate of Fluid Absorption in Porous Media*, Master's Thesis, University of Maine, Orono, ME, USA.
- Sharma, D. K., Bapat, S., Brandes, W. F., Rice, E., and Castaldi, M. J. (2019). "Technical feasibility of zero waste for paper and plastic wastes," *Waste and Biomass Valorization* 10(5), 1355-1363. DOI: 10.1007/s12649-017-0109-5
- Srivatsa, N. R., and Markham, L. D. (1993). "Postconsumer milk and juice cartons can be recycled with existing technology," *Pulp Paper* 67(8), 69-71.
- Syverud, K., and Stenius, P. (2009). "Strength and barrier properties of MFC films," *Cellulose* 16(1), 75. DOI: 10.1007/s10570-008-9244-2
- Tayeb, A., Tajvidi, M., and Bousfield, D. (2020a). "Paper based oil barrier packaging using lignin-containing cellulose nanofibrils," *Molecules* 25(6), 1344. DOI: 10.3390/molecules25061344
- Tayeb, A., Tajvidi, M., and Bousfield, D. (2020b). "Enhancing the oxygen barrier properties of nanocellulose at high humidity: Numerical and experimental assessment," *Sustainable Chemistry* 1(3), pp.198-208. DOI: 10.3390/suschem1030014
- Triantafillopoulos, N., and Koukoulas, A. A. (2020). "The future of single-use paper coffee cups: Current progress and outlook," *BioResources* 15(3), 7260-7287. DOI: 10.15376/biores.15.3.7260-7287
- Vyorykka, J., Zuercher, K., and Malotky, D. (2011). "Aqueous polyolefin dispersion for packaging boards and papers," in: TAPPI PAPERCON, Atlanta GA, USA.
- Wang, J., Gardner, D. J., Stark, N. M., Bousfield, D. W., Tajvidi, M., and Cai, Z. (2018). "Moisture and oxygen barrier properties of cellulose nanomaterial-based films," *ACS Sustainable Chemistry & Engineering*, 6(1), 49-70. DOI: 10.1021/acssuschemeng.7b03523
- Wenzel, D. J., Bartholomew, G. W., Quick, J. R., Delozier, M. S., and Klass-Hoffman, M. (International Paper Co.) (1998). "Recyclable and compostable coated paper stocks and related methods of manufacture," U.S. Patent 5,837,383.
- Zatloukal, M. (2016). "Measurements and modeling of temperature-strain rate dependent uniaxial and planar extensional viscosities for branched LDPE polymer melt," *Polymer* 104, 258-267. DOI: 10.1016/j.polymer.2016.04.053

Article submitted: December 21, 2020; Peer review completed: February 28, 2021;
Revised version received and accepted: March 15, 2021; Published: March 16, 2021
DOI: 10.15376/biores.16.2.3285-3297